

Rarefied Gas Dynamic Effects on Mass Spectrometric Studies of Upper Planetary Atmospheres

J. B. French* and N. M. Reid†
University of Toronto, Toronto, Canada

and
A. O. Nier‡ and J. L. Hayden§
University of Minnesota, Minneapolis, Minn.

Results are presented of measurements obtained with an open-source mass spectrometer both in earth orbit and in a laboratory molecular beam facility. The mass spectrometer/ion source combination was developed in the laboratory to be operable in either of two modes by altering ion extraction potential on ground command, i.e., as a stagnation cavity or to respond only to the incoming molecules of the unperturbed atmosphere. Results indicate that the use of this open-source configuration and dual-mode capability, allied with both standard static calibration and dynamic calibration using high-speed molecular beam techniques in the laboratory, allows collection of useful data on aeronomy of the upper atmosphere of planets and comet tails

Introduction

MASS spectrometry has been in use as a tool for studying aeronomy of the upper atmosphere in recent years. Mass spectrometers are mounted aboard sounding rockets and satellites to determine the concentrations of gas species in the atmosphere around the vehicle by analyzing the densities of the various species in the on-board instrument. However, the densities are strongly affected by molecular reflection processes at the spacecraft surface. The present work demonstrates that it is possible to measure the undisturbed atmospheric composition directly by utilizing retarding electric fields to discriminate effectively against reflected molecules.

The sounding rocket or satellite in general, however, causes a large perturbation to the local atmosphere, largely because of its high-speed flight but also because of vehicle outgasing. In the upper atmospheric free-molecule flow situation, the partial densities of each gas species near the instrument surface (to which a mass spectrometer responds) contain in general contributions from several classes of molecules: 1) approaching molecules of the unperturbed atmosphere. 2) partially accommodated molecules reflected after one or more collisions at the surface. 3) desorbing molecules which were adsorbed as atoms or molecules during the earlier exposure of the surface. 4) molecules produced by chemical reactions at the mass spectrometer or gage filament or by diffusion and outgasing from the instrument surfaces.

Received October 15, 1974; revision received May 20, 1975. This research was supported by the NASA Viking Project through Contract NAS 1-9697 between NASA Langley Research Center and the University of Minnesota, and NASA Grant NGL-24-055-009 to the University of Minnesota. The molecular beam facility construction was made possible by Grant A-2731 from the Canadian NRC and Grant 9551-17 from the Canadian Defense Research Board to the University of Toronto. We are indebted to R. Parsons and J. Leffers for the facility preparation and operation, to C. Lam for the molecular beam operation, to J. Ballenthin for assistance in the experiments, and to R. J. Duckett of NASA Langley Research Center for the support and encouragement of this work.

Index categories: Rarefied Flows; Spacecraft Ground Testing and Simulation (including Components).

*Associate Director, Institute for Aerospace Studies. Member AIAA.

†Research Associate, Institute for Aerospace Studies.

‡Regents' Professor, School of Physics and Astronomy.

§Senior Scientist, School of Physics and Astronomy.

The earlier measurements, in general, sought to avoid the inherent difficulties of calibrating instrument response to this multimodal velocity distribution function at the exposed vehicle surface, by utilizing a cavity or orifice gage in which the incident population can be relaxed to a Maxwellian distribution. In the ideal case (no surface adsorption, no chemical reaction) the density in the gage cavity n_g at temperature T_g can be readily related to free atmospheric density n_0 , temperature T_0 and speed ratio S by¹

$$V(dn_g/dt) = (A_0 n_0 c_m / 2\sqrt{\pi}) \exp[-(S \cos \pi)^2] + (S \cos \psi) \pi (1 + \operatorname{erf} S \cos \psi) - A_0 (n_g c_m / 4) \quad (1)$$

where A_0 is the area of the knife-edge orifice, V is the gage volume, c_m is the most probable random speed, and ψ is the angle between the normal to the gage orifice and the flight vector. For a slowly spinning satellite, where the volume time constant of the gage $4V/c_m A_0$ is small compared to the period of rotation, Eq. (1) would predict a) a ram density when gage facing directly into the flow typically an order-of-magnitude greater than ambient, b) the simple thermal transpiration result when $\psi = 90^\circ$, and c) an extremely low wake density when $\psi = 180^\circ$. It was usually found, however, that apparent wake density remained much higher than expected, due to outgasing.

At first this reading was subtracted for the whole spin cycle, but Moe and Moe² correctly pointed out that, under long-term equilibrium, net desorption during one part of the cycle meant net adsorption in another part, so the correction to ram density should be additive rather than subtractive. The situation was first approximated in analyzing data from Explorer XVII by utilizing the simple Langmuir adsorption model, where A_w is the gage wall area, θ is the fraction of the wall covered by adsorbed gas, α is the probability of sticking on the bare surface, and ν is the molecular desorption rate per cm^2 per sec from the covered area. Equation (1) then becomes, using the same function of S and ψ ,

$$V(dn_g/dt) = (A_0 n_0 c_m / 2\pi) F(S, \psi) - [A_0 + A_w (1 - \theta) \alpha] (n_g c_m / 4) + A_w \nu \theta \quad (2)$$

Even with this primitive model, physically reasonable values of α and ν can be used which yield a density-time curve similar to that observed. The treatment was later extended,³ in

analyzing data from the Spades satellite, to a "patch" model in which patches of the various atmospheric gases were assumed to be adsorbed, to account for surface heterogeneity and the atmospheric gas mixture. This allows for desorption/adsorption phenomena with time constants of hours (which show up as an apparent density hysteresis over one orbit) as well as for the shorter time (which dominate spin hysteresis). However, the complexity of the model is more suited to the more complex information obtainable when a mass spectrometer is used. The corrections implied to the inferred aeronomic data can be sizable (up to 30%), but still do not provide a match to densities inferred from other measurements such as orbital decay, as they do not take into account factors such as the loss of atomic oxygen by reaction at the wall.

Perhaps the most sophisticated analysis yet of the effect of surface interactions is that provided by Hedin et al.,⁴ in which a mass spectrometer was employed with a cavity geometry for the ion source region. In addition to adsorption/desorption processes for the atmospheric gases, the analysis takes into account production of CO and CO₂ by wall reactions of atomic oxygen with surface carbon as well as recombination of atomic oxygen. The analysis, which involved fitting the data to an assumed atmospheric model, showed that the surface properties become stabilized after a few weeks. All oxygen in the atmosphere was measured as O₂, but only after the first few weeks was the loss of O through formation of CO and CO₂ small enough to be neglected in the atmospheric oxygen density inferred. The mass 28 peak was dominated by CO rather than atmospheric N₂, and was still decreasing after a year in orbit.

The inference that surfaces aged in orbit are effective at recombining O to O₂ but do not cause significant loss via reactions with carbon was used by Newton et al.⁵ for analyzing data from the San Marcos 3 satellite during its last orbits, and good agreement between this inferred density and that inferred from drag was obtained.

In summary, it may be said that, while much valid aeronomic information has been inferred from the data from cavity instruments, they suffer from limitations due basically to the fact that the gas population in the ion source is strongly modified by surface interactions. All information concerning active species is obtained by inference rather than directly. Characteristic time constants for the various desorption processes, and surface coefficients which vary as the surfaces age make interpretation difficult. This is especially true during the first weeks in orbit, making this approach particularly unsuitable for missions requiring fast response over many decades of density, for instance, rocket probes, one-shot planetary entry probes, and comet-tail flythroughs.

These difficulties have led to several proposals and experiments involving the more open ion source, which gives much faster response and sensitivity to active species, but for which the problem of the incompletely accommodated reflected molecules must be faced. Perhaps the earliest experiments were the forward-facing open source flown by Schaefer,⁶ the first to detect atomic oxygen. Rocket flights involving open sources include the various rocket probes of Nier et al.,⁷ the side focusing quasi-open ion source used by Niemann et al.⁸ and the helium-cooled ion source used by Offermann and Trinks.⁹

In the configurations used in the first two of these, the open sources responded to a mixture of incident and reflected molecules. In the method of Ref. 7, comparison is made between an open-source mass spectrometer and two other mass spectrometers with cavity geometry ion sources, which thus permit a calibration of the open source with respect to the inactive gases at least. The method used by Niemann et al.⁸ was to analyze the data by noting the changing relative densities of the reflected and approaching stream of molecules as attitude varied due to spin. Using the simple Maxwell model to split the reflected molecules into specular and diffuse frac-

tions allowed computation of partial densities vs altitude for various attitudes which could be made self-consistent with physically reasonable choices of the fraction coefficient. The atomic oxygen data could not be made consistent without recourse to a more complex surface adsorption model.

These instruments and others, both rocket and satellite mounted, have all contributed greatly to the knowledge of the earth's upper atmosphere. One of the most difficult aspects of this research has been the resolution of uncertainties concerning the atomic to molecular oxygen ratio. It may be stated that all of these techniques use inferential methods to determine the absolute amounts of each species, and none provide a direct simple method that can be used with confidence to study diurnal variations and other aeronomic phenomena.

The method used by Offermann and Trinks⁹ is the only one to attempt to remove totally the uncertainties due to reflected molecules by the direct physical means of cryopumping the incident stream. This elegant approach, when the instrument laboratory calibration is performed using an adequate energy, composition, and speed ratio simulation of the in-flight case, provides a direct measurement of the absolute atmospheric partial densities. Its only limitations are that it does not permit the possibility of utilizing the ram enhancement gain in sensitivity, which can be useful in measuring the inactive gases in extremely rarefied conditions, and the obvious practical limitations for use in orbit and deep space probes.

Dual-Mode Open-Source Mass Spectrometer

Laboratory studies were undertaken of an ion source configuration which could hopefully overcome the previously discussed shortcomings, by operating either as a true flythrough instrument responsive only to incident molecules, or as a close (i.e., calibratable) approximation to a cavity or stagnation instrument.

The basic concept was to utilize the difference in the directed kinetic energy of the incident and reflected particles to distinguish between them. This idea has been suggested but never attempted before,¹⁰ but it was the combination of the particularly well-suited Nier-source geometry and the availability of the high-speed molecular beam which made the

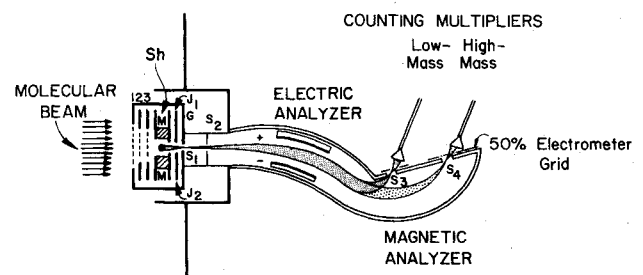


Fig. 1 Ion source and mass spectrometer schematic.

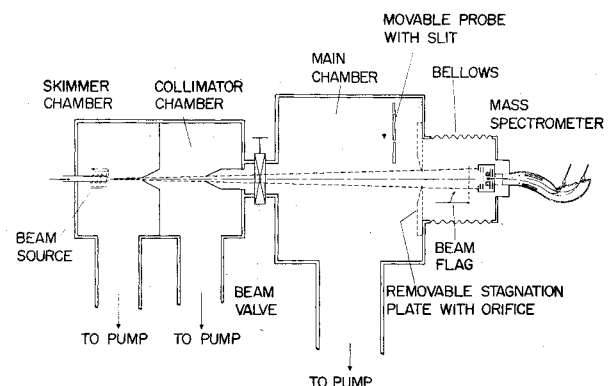


Fig. 2 Molecular beam simulation system.

present study feasible. The mass spectrometer and ion source geometry is shown schematically in Fig. 1.

The source consists of a magnetically confined electron beam traversing an open cup-shaped cavity with an ion exit slit in the bottom about equal to the electron beam width. The electron beam current was, typically, 100 microamps, leading to a space charge depression of no more than 0.2v. In the normal operating mode the J plates apply a sufficient field strength to extract all ions formed in the electron beam. The ion signal is then proportional to the molecular density in the electron beam pencil, regardless of molecular direction or energy spread since the double focusing Mattauch-Herzog geometry used is relatively insensitive to angular or energy spread of the ion source.

The alternate mode investigated was to set the potential of the elements surrounding the electron beam almost equal, thus relying on the kinetic energy of the incident particles to carry them through the extraction slit S_1 . This mode was termed the "retarding mode" because it was realized that small fields to form a slight retarding barrier might be necessary to reject ions formed from desorbed molecules or even from partially accommodated reflected molecules. The results presented are from the optimum selection of potentials.

The instrument was studied in a molecular beam facility described in earlier papers^{11,13}. It is shown schematically in Fig. 2. Relatively high-speed ratio (i.e., monoenergetic) beams of various gases were produced by a heated, seeded nozzle beam source and measured for velocity distribution and composition by instruments in the main chamber (not shown). The test instrument was mounted so that the beam fully illuminated the source aperture, and could be pitched and yawed on a bellows-sealed gimbal. The movable stagnation plate and beam flag shown allowed the conditions given in Table 1 to be studied.

Ideal stagnation is the condition where the instrument reads only the fully randomized population in a large cavity with a knife-edged orifice. Figure 3(a) and (b) shows typical spectra, using the ion source in its normal (or stagnation) mode, taken at 3.9 km/sec beam velocity with argon and CO₂ as an approximation to the Viking Martian entry, in which this instrument will also be used. Note the large ratios of beam to background (A to B) for the parent and daughter (fragment) peaks of the beam gases, a result of the high intensity beam (approximately 10^{13} molecules/cm² sec) and large pump speed available (10000 liters/sec). Facility background gases (e.g., oxygen at 32) are invariant. Earlier work using this technique¹¹ had established that the ion source cup should have a depth to diameter ratio of about one to yield a good ram enhancement of signal, yet not be overly sensitive to pitch and yaw rolloff. Detailed measurements taken from data such as Fig. 3 showed that at high beam velocities the ratio of ef-

fective stagnation to ideal stagnation was about 0.96 for the stable gases such as N₂, O₂, Ar and CO₂. This happens to correspond closely to the result obtained if the incident molecules reflect from the bottom with cosine distribution and complete accommodation, although this is not likely in reality. Helium, on the other hand, gave about 77% of ideal stagnation, corresponding to much poorer accommodation, as expected.

Figure 4 shows, in comparison, the best ratio of incident to reflected molecule signals achieved by adjusting source potentials as described. F_A and F_B are "flythrough A" and "flythrough B" modes, respectively. F_B shows that, when the flag is in place, no observable signal for argon or CO₂ is present, i.e., the reflected molecules are not "seen" at all. In Fig. 4, F_A is less than half A in Fig. 3a because of this loss in signal corresponding to the reflected molecules. Fragment ions from CO₂ (at 28, 16, and 12) are still seen because of their recoil energies.

The capability to distinguish between incoming and reflected molecules is illustrated more explicitly in Fig. 5 for

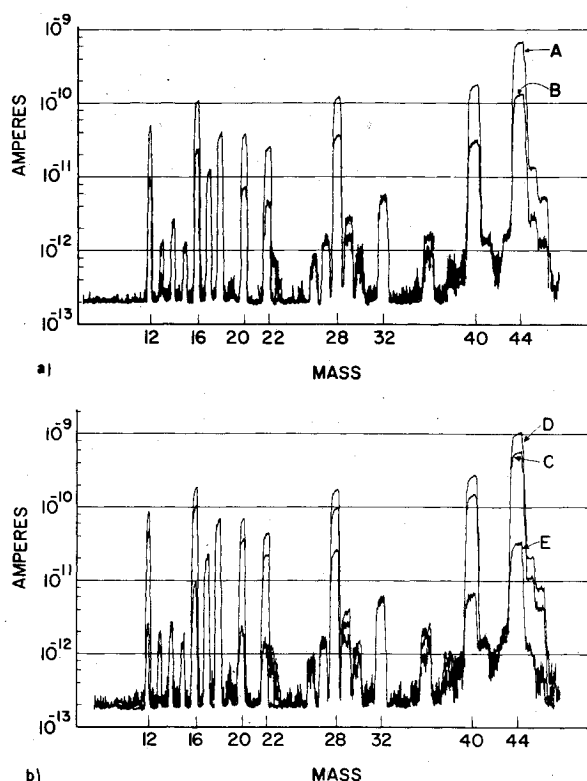


Fig. 3 Typical mass spectra, for a 3.9 km/sec He, Ar, CO₂ stagnation mode. a) Normal source mode. b) Ion source region in stagnation mode.

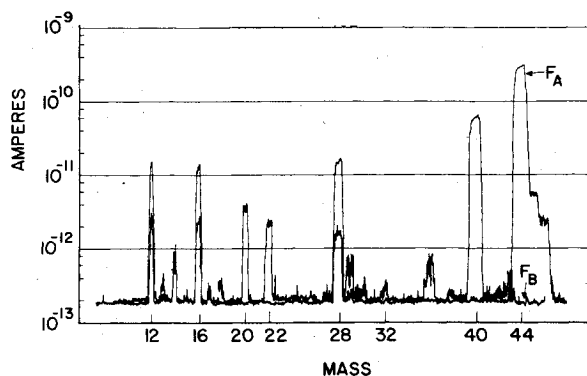


Fig. 4 Spectra obtained with the same beam, retarding mode. CO₂-Ar-He mixture, 3.9 km/sec beam velocity.

Table 1 Conditions and their interpretation

	Condition	Interpretation
A-	Beam unflagged, no stagnation plate	Simulated flight signal plus local background near instrument
B-	Beam flagged, no stagnation plate	Local background near instrument
C-	Stagnation plate, beam flagged	"Ideal" cavity stagnation plus main chamber background
D-	Stagnation plate, beam unflagged	Maximum simulated flight signal if ideally stagnated, plus main chamber background
E-	Beam flagged in main chamber	Main chamber background pressure

Then $(A - B)$ = simulated flight signal

$(A - B)/(C - E)$ = ratio of flight signal to signal corresponding to ideal stagnation

argon, again at 3.9 km/sec. In this experiment, the slit mask, which produced a narrow ribbon beam of incident molecules, was moved across the source region. In the retarding mode, only when incident molecules are passing through the electron beam is there any appreciable signal present.

Argon atoms at 3.9 km/sec possess 3.2 eV of kinetic energy; the technique can, therefore, be assumed to be applicable to all gases measured in earth orbit or planetary entry conditions, except helium or hydrogen. Actually, very high incident to reflected ratios were achieved for helium also.

For comparison with the orbital data covered later, Fig. 6 illustrates the sharp falloff in the argon and CO₂ retarding mode signal for rotation of the ion source perpendicularly to

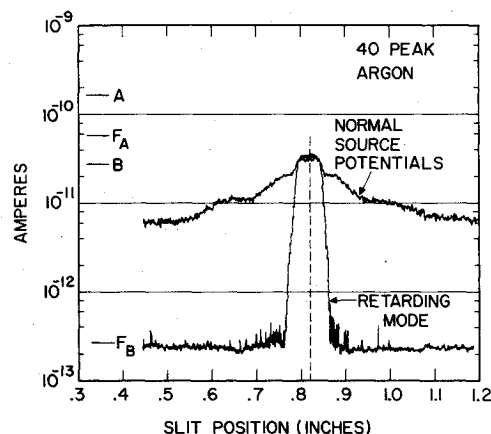


Fig. 5 Scan of ion source with ribbon beam produced by movable slit mask.

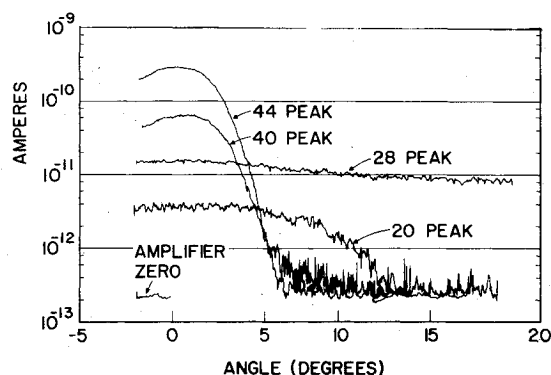


Fig. 6 Instrument response to angular rotation, retarding mode. CO₂-Ar-He mixture, 3.9 km/sec beam velocity. Rotation perpendicular to electron beam.

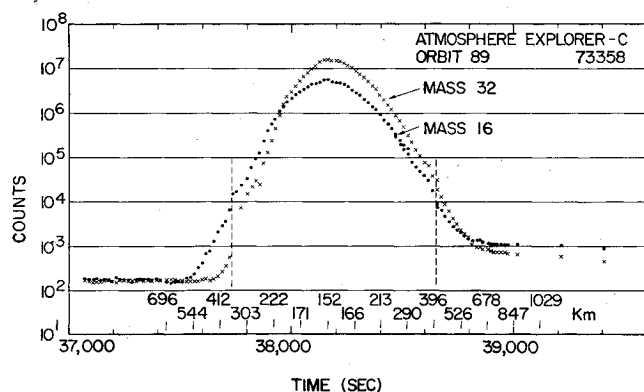


Fig. 7 Response of dual-mode mass spectrometer during orbit 89, the first orbit that the instrument was exposed to atmosphere-stagnation mode.

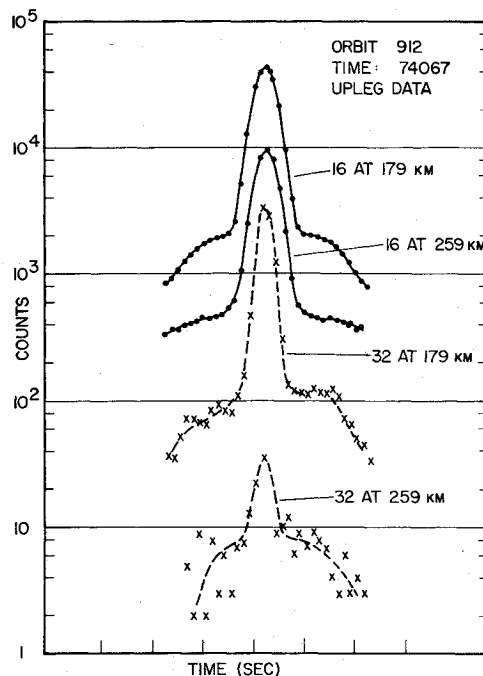


Fig. 8 Orbit data in retarding mode, from portion of spin cycles at 179 and 259 km.

the electron beam. Thus, with a molecular beam possessing almost no transverse energy, the instrument response drops to almost zero with 6° of angle. This calibration can be used to determine the kinetic temperature directly for gases observed in orbit.

Orbital Data From Dual-Mode Open-Source Mass Spectrometer

Because of these very promising results, an almost identical mass spectrometer being flown by two of us¹ on the atmospheric Explorer C satellite was modified, so that it could be switched by ground command between the two modes. Available potentials did not permit the optimum retarding mode tuning obtained in the laboratory. The complete aeronomic data will be reported elsewhere; we include here some of the early analyzed data to illustrate the main contentions of this paper.

Figure 7 illustrates the very interesting data obtained during the first orbit (89) in which the ion source was exposed to ambient conditions and operated only in the conventional stagnation mode. The satellite was spinning slowly and the data points correspond to maximum ram pressure. As the satellite descended toward perigee, only mass 16 was observed down to about 400 km, that is, no atomic oxygen was being reflected or re-emitted in the source as O₂. However, after the one perigee exposure the source surface conditions had changed, with long time-scale desorption of both O₂ and O. Subsequent orbits revealed that the surface had become much more catalytic for atomic oxygen recombination, and showed strong asymmetry in the CO₂ peak, thus corroborating the loss mechanism suggested by the OGO-6 data.

In later orbits, the instrument worked alternately in the stagnation mode and the retarding mode. Figure 8 shows data for mass 16 and 32 taking in the retarding mode at two altitudes as a function of the spin cycle, where motion between data points corresponds to 3° of spin about an axis perpendicular to the electron beam. Comparing this to Fig. 6 obtained in the laboratory, it is clear that, while the rejection of reflected species is not as complete as in the laboratory tests (due to the unoptimized potentials used), the large peak solely

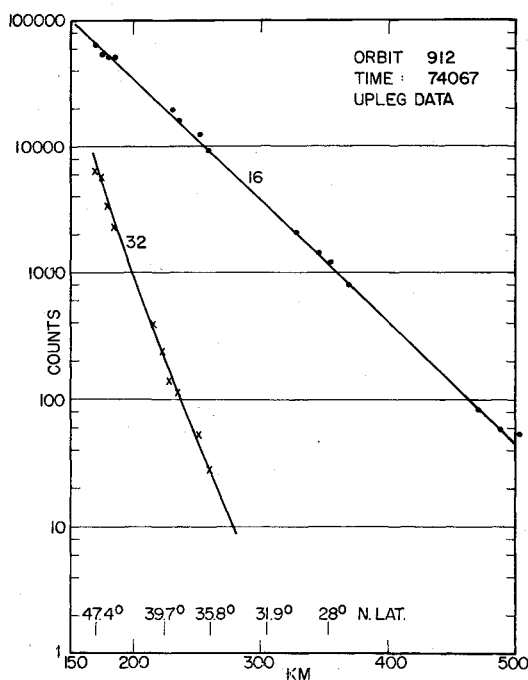


Fig. 9 O and O₂ variation with altitude.

due to incident molecules is clearly separable. (In the laboratory and orbital measurements in this mode the electron beam energy was reduced to 25 eV from 75 eV, to reduce the relative contribution at mass 16 from the ion fragment from mass 32.) Note the large ratio of O/O₂ at both altitudes. The peak width of the O is greater than the O₂, due to thermal broadening. In fact, by taking the laboratory calibration in Fig. 6 as the width produced by a gas with almost no transverse energy spread (about 12° shoulder-to-shoulder for mass 40), the very significant extra width for mass 32 at 179 km can be used (beyond that attributable to the lighter mass) to calculate the kinetic temperature directly, very useful extra information to compare to temperature inferred from scale height data.

The altitude variation of 16 and 32, from many such peaks as in Fig. 8, is shown in Fig. 9. This is the first data from a satellite mass spectrometer which shows O as O and O₂ as O₂, from which the O/O₂ ratio can be calculated directly. Scale heights taken from these data are not too meaningful, as latitude variation is mixed in, but the slopes and ratio are as expected.

There is a vast amount of more data of aeronomic interest waiting to be analyzed from this experiment, including information on other gases such as He and H₂. However, the analysis to date has shown the strong advantages of the dual-mode orbital capability associated with dynamic and static laboratory calibration. Perhaps the best way of summarizing this is to list the stages in the calibration and orbital data analysis procedures evolved.

Calibration for N₂

1) The static calibration (ion count rate for known source density of that species) is obtained by using conventional laboratory calibration for several atmospheric gases, for both 75 eV and 25 eV electron beam energies.

2) Dynamic calibrations for the various atmospheric gases are obtained by using the fast molecular beam techniques shown in Fig. 2, at both 75 eV and 25 eV electron beam energy. The stagnation plate technique allows laboratory determination of the incident flux and hence the calibration of the instrument response operating in either the stagnation or the retarding (flythrough) mode. In-flight number density is known, since the beam velocity is accurately measured in-

dependently.¹¹ For the present results, parts of this calibration procedure have not been completed as yet.

3) The stagnation factor for the source is now known. (For all gases but helium, this was about 96% of ideal; helium was 77%. This factor was almost invariant from 1 to 4 km/sec, and is assumed to hold at the 8.5 km/sec earth orbital velocity.) Then from raw data such as in Fig. 7 for mass 28, ambient nitrogen density vs altitude is determined. Interference from CO at 28 is negligible at all but the highest altitude, and is determined by noting the 14 peak height, which is only related to nitrogen.

4) In some orbits during which the instrument was alternated between the stagnating and flythrough mode, the flythrough segments can be graphically interpolated, thus providing a direct in-flight calibration of the instrument response to flythrough number density of nitrogen, or a ratio of flythrough to stagnation mode response to nitrogen. This calibration can be cross-checked against the laboratory molecular beam calibration.

Calibration for O₂ and O

This calibration is complicated by the fact that, at all altitudes at which the satellite flew, significant atomic oxygen is present.

1) Assume that the ratio of flythrough mode to stagnation mode response determined above for nitrogen carries over to O₂. (This assumption can be cross-checked in the laboratory molecular beam calibration without atomic oxygen being present). Then the orbital flythrough mode response is used to calculate orbital O₂ density vs altitude (because the stagnation mode response is complicated by the recombined atomic oxygen in the source).

2) Note that at this point flythrough mode responses and ambient densities of the N₂ and O₂ are known. Thus, any discrepancies which may occur in the stagnation mode results due to the surface adsorption/desorption effects described earlier can be examined independently, and used to correct the stagnation mode results where desired (for example, for extrapolation to altitudes where the flythrough mode signal is too weak).

3) To determine the altitude variation of atomic oxygen, the laboratory molecular beam flythrough mode calibration can be used directly. Alternately, the signal obtained at altitudes where all oxygen is present in the atomic form can be used. Once the source is aged by orbital exposure, it is now known that the stagnation mode response is dominated by oxygen recombined to O₂. There is a correction due to the density of the incident atomic oxygen, which can be estimated. This stagnation mode data can then be used to determine atomic oxygen number density vs altitude.

4) Using orbits for which flythrough and stagnation mode response are interspersed, the flythrough mode response for atomic oxygen can be cross-checked with the laboratory calibration. Then all calibration data are available to determine O and O₂ variation with altitude.

5) The procedure for other gases (He, H₂, Ar, CO₂ water vapor) is similar, and in all cases effects due to instrument gas-surface interactions can be examined explicitly.

Conclusions

The steady evolution of understanding of the complexity of the gas-surface interactions and their influence on aeronomic measurements has caused a similar evolution in the design of instruments and in the analysis of orbital data. While a great amount of valuable data has been produced, this complexity of surface interaction means that the measurements are generally indirect. The present approach, in which the effects of surface interactions can be eliminated or included at will, circumvents the problems associated with surface effects. This permits, for the first time, an instrument which can 1) have

the fast response and sensitivity for active gases required for future planetary probes, 2) obtain direct data on the undisturbed ambient atmosphere without interference from reflected species, 3) at the same time retain the advantages of ram enhancement of signal and stagnation calibration for stable gases, to be invoked when advantageous, and 4) obtain explicit data on the gas-surface interactions occurring.

References

- ¹Patterson, G. N., "Mechanics of Rarefied Gases and Plasmas," Rev. 18, Institute for Aerospace Studies, University of Toronto, 1964.
- ²Moe, K. and Moe, M. M., "The Roles of Kinetic Theory and Gas Surface Interactions in Measurements of Upper Atmospheric Density," *Planetary Space Science*, Vol. 17, 5, May, 1969, pp. 917-922.
- ³Moe, K., Moe, M. M., and Yelaca, N. W., "Effect of Surface Homogeneity on the Adsorptive Behavior of Orbiting Pressure Gauges," *Journal of Geophysical Research*, Vol. 77, Aug. 1972, pp. 4242-4247.
- ⁴Hedin, A. E., Hinton, B. B., and Schmitt, G. A., "Role of Gas Surface Interactions in the Reduction of OGO 6 Neutral-Particle Mass Spectrometer Data," NASA TN D-7239, March 1973.
- ⁵Newton, G. P., Kasprzak, W. T., and Pelz, D. T., "Equatorial Composition in the 137- to 225-km Region from the San Marco 3 Mass Spectrometer," *Journal of Geophysical Research*, Vol. 79, May 1974, pp. 1929-1941.
- ⁶Schaefer, E. J., "The Dissociation of Oxygen Measured by a Rocket-Borne Mass Spectrometer," *Journal of Geophysical Research*, Vol. 68, Feb. 1963, pp. 1175-1176.
- ⁷Nier, A. O., "Measurement of Thermosphere Composition," *Space Research*, Vol. XII, Adademi-Verlag, Berlin, Nov., 1972, pp. 881-889.
- ⁸Niemann, H. B., Spencer, N. W., and Schmitt, G. A., "A Thermosphere Composition Measurement Using a Quadrupole Mass Spectrometer with a Side Energy Focusing Quasi-Open Source," *Journal of Geophysical Research*, Vol. 78, May 1973, pp. 2265-2277.
- ⁹Offermann, D. and Trinks, H., "A Rocket-Borne Mass Spectrometer with Helium-Cooled Ion-Source," *Review of Scientific Instruments*, Vol. 42, Dec. 1971, pp. 1836-1843.
- ¹⁰Philbrick, C. R., Narcisi, R. S., Baker, D. W., Trzcinski, E., and Gardner, M. E., "Satellite Measurements of Neutral Composition with a Velocity Mass Spectrometer," *Space Research*, Vol. XIII, Apr., Akademie-Verlag, Berlin, 1973, pp. 321-325.
- ¹¹French J. B., Reid, N. M., Nier, A. O., and Hayden, J. L., "Molecular Beam Simulation of Planetary Atmospheric Entry - Some Recent Results," *CASI Transactions*, Vol. 5, Sept. 1972, pp. 77-82.
- ¹²Nier, A. O., Hayden, J. L., French, J. B., and Reid, N. M., "On the Determination of Thermospheric Atomic Oxygen Densities with Rocket-Bourne Mass Spectrometers," *Journal of Geophysical Research*, Vol. 77, 10, Apr., 1972, pp. 1987.
- ¹³Nier, A. O., Hayden, J. L., French, J. B., and Reid, N. M., "Measurement of Neutral Atmospheric Composition with Mass Spectrometers Carried on High-Speed Vehicles," *EOS: Transactions, American Geophysical Union*, Vol. 54, 11, Nov., 1973, pp. 1146.

From the AIAA Progress in Astronautics and Aeronautics Series . . .

STRATOSPHERIC CIRCULATION—v. 22

Edited by Willis L. Webb, White Sands Missile Range, and University of Texas at El Paso

Thirty papers in this volume present data from synoptic rocket exploration of the stratosphere, disclosing fundamental circulation, and tidal and global circulation systems.

A summary of stratospheric circulation is presented, detailing the state of knowledge and the Meteorological Rocket Network (MRN) and the development of the Stratospheric Circulation Index (SCI), with the outlook for a global sounding rocket network.

Covers the British Skua rocket system, the Polish Meteor-I, the Air Force PWN-8B (Loki-Dart) and ARCAS meteorological rockets, and the Kookaburra dropsonde rocket system.

Examinations of meteorological sensing systems cover radar chaff, parachute-borne sensors, balloon sounding, resistance wire and thermistor use in temperature sensing, and ozonesondes.

Atmosphere studies cover clouds, mesospheric ozone, and a photochemical model of the mesosphere. Upper atmosphere studies cover specific geographic areas and upper atmosphere climatology; comparing current data with previous studies and the Standard Atmosphere Supplements.

600 pp., 6 x 9, illus. \$18.00 Mem. & List

TO ORDER WRITE: Publications Dept., AIAA, 1290 Avenue of the Americas, New York, N. Y. 10019